



저작자표시-비영리-변경금지 2.0 대한민국

이용자는 아래의 조건을 따르는 경우에 한하여 자유롭게

- 이 저작물을 복제, 배포, 전송, 전시, 공연 및 방송할 수 있습니다.

다음과 같은 조건을 따라야 합니다:



저작자표시. 귀하는 원저작자를 표시하여야 합니다.



비영리. 귀하는 이 저작물을 영리 목적으로 이용할 수 없습니다.



변경금지. 귀하는 이 저작물을 개작, 변형 또는 가공할 수 없습니다.

- 귀하는, 이 저작물의 재이용이나 배포의 경우, 이 저작물에 적용된 이용허락조건을 명확하게 나타내어야 합니다.
- 저작권자로부터 별도의 허가를 받으면 이러한 조건들은 적용되지 않습니다.

저작권법에 따른 이용자의 권리는 위의 내용에 의하여 영향을 받지 않습니다.

이것은 [이용허락규약\(Legal Code\)](#)을 이해하기 쉽게 요약한 것입니다.

[Disclaimer](#)

가

Entrance and Run Angles Variation Method
of Hull Form Preserving the Prismatic
Coefficient

가

2022 2

심사위원	신	동	목	안
심사위원	오	민	재	오민재
심사위원	안	형	택	안형택

가

Offset , Lines ,
2D lines
.
.
.
가 Free-Form
Deformation . Free-Form Deformation
. Free-Form Deformation
.
가 .
가 Free-Form Deformation
가
가 $1 - C_P$
.
.
가 .
가 .

1	-----	1
1.1	-----	1
1.2	-----	2
1.2	-----	3
2	-----	4
2.1 Free-Form Deformation	-----	4
2.2 $C_P(\quad)$	-----	6
2.2.1 C_P variation	-----	7
3	-----	10
3.1	-----	10
3.2	-----	11
3.3 C_P	-----	12
3.4 Free-Form Deformation LBD	-----	13
3.5 $1-C_P$	-----	16
3.5.1 $1-C_P$	-----	16
3.6 가 ,	-----	19
3.6.1 가 , FFD	-----	20
3.7 Local $1-C_P$	-----	23
3.7.1 Local $1-C_P$	-----	26
3.7.2 Local $1-C_P$	-----	28
4	-----	31

Fig 1.1 Hull form variation proceed	1
Fig 2.1 Original and variated Min–Max Box	4
Fig 2.2 Original and variated Min–Max Box's control points	5
Fig 2.3 Prismatic coefficient	6
Fig 2.4 Generate new C_P curve for design ship	7
Fig 2.5 Definition of each section's longitudinal shift in $1-C_P$ variation	8
Fig 3.1 Flow chart of the proposed hull form variation method	10
Fig 3.2 KCS offset data	11
Fig 3.3 Generating midship section line	11
Fig 3.4 Make curve from offset data	12
Fig 3.5 The offset where curve and plane meet	12
Fig 3.6 The method of calculating C_P	12
Fig 3.7 The method of calculating Sectional Area Curve	13
Fig 3.8 KVLCC2 applying 99.7% LBD FFD variation	16
Fig 3.9 KVLCC2 after $1-C_P$ correction	16
Fig 3.10 Comparison C_P curve before and after $1-C_P$ correction	17
Fig 3.11 KVLCC2 applying 100.5% LBD variation	17
Fig 3.12 KVLCC2 after $1-C_P$ correction	18
Fig 3.13 Comparison C_P curve before and after $1-C_P$ correction	18
Fig 3.14 Run angle and entrance angle	19
Fig 3.15 FFD method of entrance angle	20
Fig 3.16 Calculation of the moved offset	21
Fig 3.17 Run angle before and after applying FFD	22
Fig 3.18 Entrance angle before and after applying FFD	22
Fig 3.19 Original $1-C_P$ variation and local $1-C_P$ variation	23
Fig 3.20 Local $1-C_P$ variation at forebody	25
Fig 3.21 Increase entrance angle and run angle after applying FFD	26
Fig 3.22 KVLCC2 corrected with Local $1-C_P$	27
Fig 3.23 Decrease entrance angle and Run angle after applying FFD	27
Fig 3.24 KVLCC2 corrected with local $1-C_P$	27
Fig 3.25 KVLCC2 corrected by local $1-C_P$ after applying 105% FFD	28

Fig 3.26 KVLCC2 corrected by local $1 - C_P$ after applying 95% FFD	28
Fig 3.27 KVLCC2 corrected by local $1 - C_P$ after applying 150% FFD	29
Fig 3.28 KVLCC2 corrected by local $1 - C_P$ after applying 200% FFD	29

Table 3.1 KVLCC2 applying LBD variation -----	14
Table 3.2 KCS applying LBD variation -----	15
Table 3.3 Compare C_p at 3.7.1 -----	29
Table 3.4 Compare C_p at 3.7.2 -----	29

1

1.1.

Fig 1.1 .
 Database (, , (Length, L),
 (Breadth, B), (Depth, D),) 가
 2D lines , lines
 .

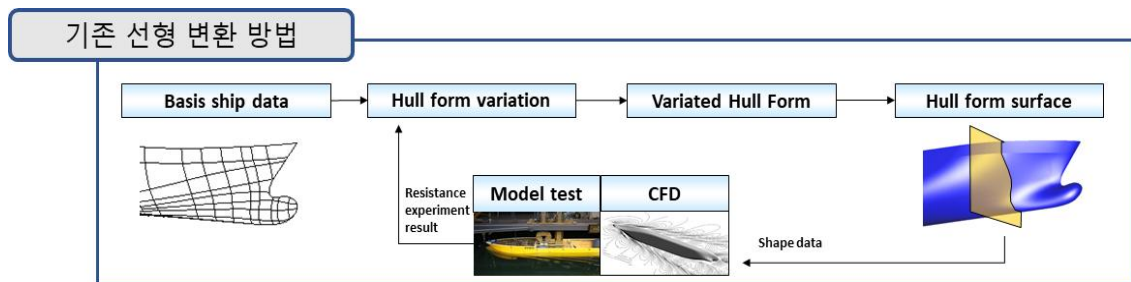


Fig 1.1 Hull form variation proceed

가 , 가
 .
 .
 , 가
 .
 (L, B,
 D, (C_P)) .

가 .

가 .

가

가

가

가

1.2.

가

가

, Free-Form Deformation [1]

. Free-Form Deformation

Local $1-C_P$

가

1.3.

, [3].
 (C_P) (Longitudinal Center of Buoyancy, LCB),
 가 ,
 .
 $1-C_P$ [2], Lackenby [4], swing .
 (Sectional Area Curve)
 section . $1-C_P$ Lackenby
 $1-C_P$ 가 Lackenby
 가 . swing .
 , [5,6,7,8,9,10,
 11,12]. [13] FOBFC(Fairness Optimized B-spline Form
 parameter Curve)
 ,
 . [14] 가
 (VOB)
 . [15]
 [16]
 [17]
 가 , LBP(Length Between
 Perpendicular) . LBP가 $1-C_P$
 C_P 가 .
 FFD
 가 , $1-C_P$.

2

2.1. Free-Form Deformation(FFD)

T.Sederberg가 Free-Form Deformation [1].

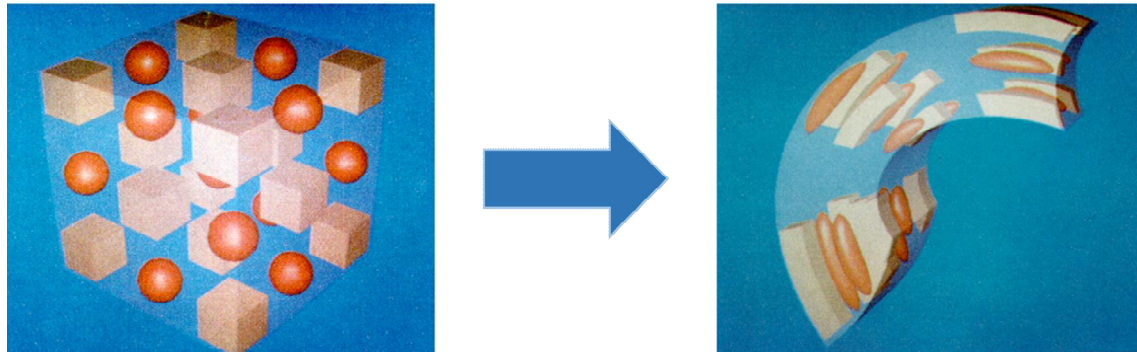


Fig 2.1 Original and varied Min-Max Box[1]

Free-Form Deformation Min-Max Box Fig 2.1, Bernstein Min-Max Box Fig 2.1 Min-Max Box (1) (s, t, u) 가 Min-Max Box (2) (s, t, u) .

$$X = X_0 + sS + tT + uU \quad (1)$$

$$s = \frac{T \times U \cdot (X - X_0)}{T \times U \cdot S}, t = \frac{S \times U \cdot (X - X_0)}{S \times U \cdot T}, u = \frac{S \times T \cdot (X - X_0)}{S \times T \cdot U} \quad (2)$$

Min-Max Box s, t, u $0 < s < 1, 0 < t < 1, 0 < u < 1$.

Min-Max Box P_{ijk} . Fig 2.2 (control point) (3) .

$$\mathbf{P}_{ijk} = \mathbf{X}_0 + \frac{i}{l}\mathbf{S} + \frac{j}{m}\mathbf{T} + \frac{k}{n}\mathbf{U} \quad (3)$$

Free-Form Deformation Min-Max Box

. Min-Max Box ,

$$\mathbf{X}_{\text{ffd}} \quad (2) \quad (s, t, u) \quad , \quad (4)$$

Bernstein . \mathbf{P}_{ijk} Bernstein .

$$\mathbf{X}_{\text{ffd}} = \sum_{i=0}^l \binom{l}{i} (1-s)^{l-i} s^i \left[\sum_{j=0}^m \binom{m}{j} (1-t)^{m-j} t^j \left[\sum_{k=0}^n \binom{n}{k} (1-u)^{n-k} u^k \mathbf{P}_{ijk} \right] \right] \quad (4)$$

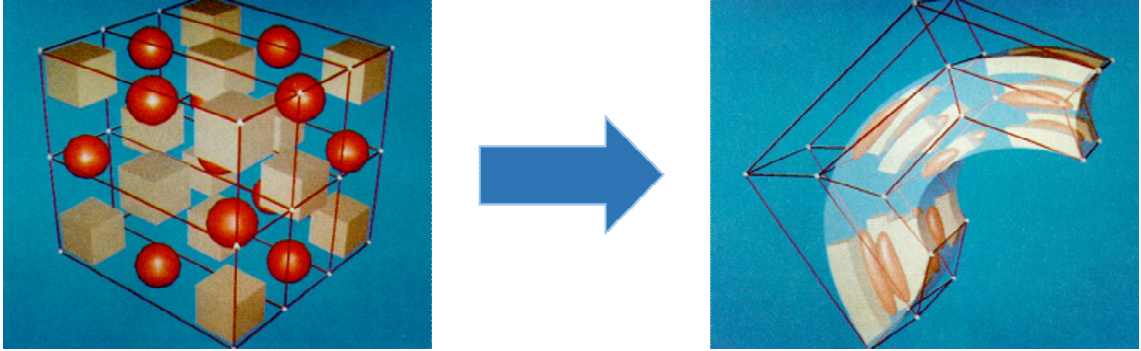


Fig 2.2 Original and varied Min-Max Box's control points[1]

2.2. C_P ()

C_P

Fig 2.3

(5)

(∇)

(L)

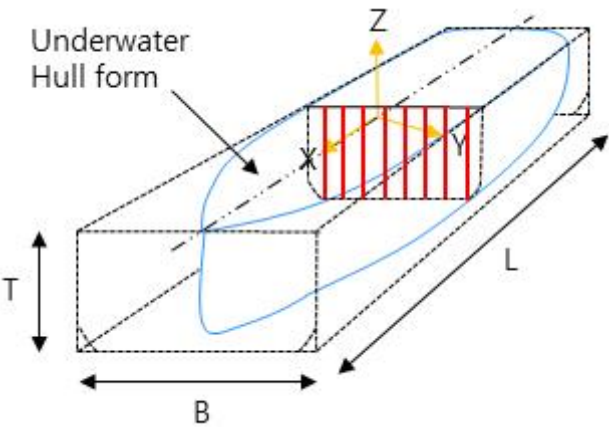


Fig 2.3 Prismatic coefficient

$$C_p = \frac{\nabla}{L \cdot A_M}$$

(5)

(5)

A_M

($L \cdot A_M$)

($L \cdot B \cdot T$)

2.2.1 C_P variation

C_P section
 LCB(Longitudinal Center Buoyancy)
 Fig 2.4 section
 C_P 2.6 (LBP)
 ± 1

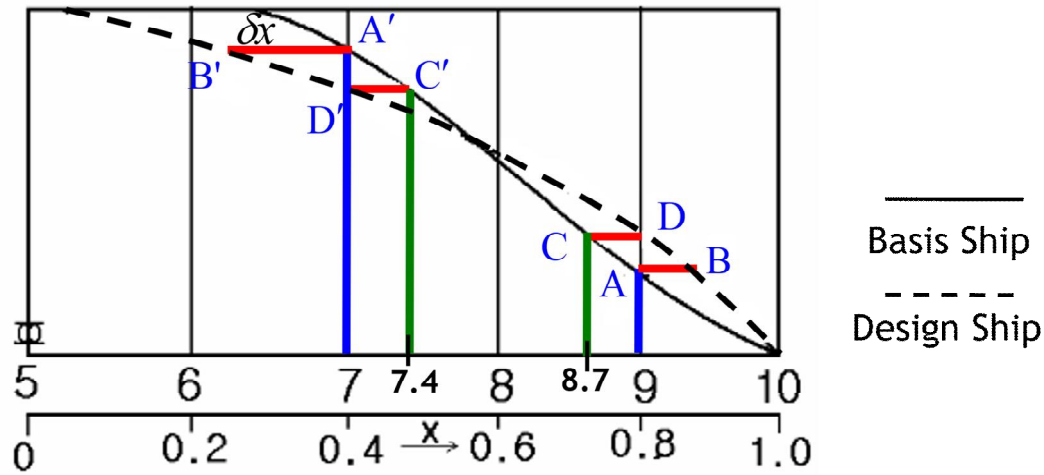


Fig 2.4 Generate new C_P curve for design ship[2]

C_P $1 - C_P$ [2], Lackenby [4], Swing station
 $1 - C_P$, Lackenby LCB
 swing station LCB
 $1 - C_P$

$1 - C_P$ (C_P) LCB
 (δC_P) LCB (δLCB) ,
 section $(\delta x_{f,a})$, Fig 2.5
 section section
 (6)

$$1 - (x_{f,a} + \delta x_{f,a}) : 1 - x_{f,a} = 1 - (C_{Pf,a} + \delta C_{Pf,a}) : 1 - C_{Pf,a} \quad (6)$$

$$\delta C_{Pf,a} \qquad h_f \quad h_a \qquad (10) \qquad .$$

$$h_{f,a} \cong \frac{C_{Pf,a}(1-2\overline{x_{f,a}})}{1-C_{Pf,a}} \qquad (10)$$

$$\begin{array}{l} \text{Free-Form Deformation} \\ C_B, \text{ LCB }, C_{WP} \qquad . \qquad \text{Volume} \\ 1-C_P \qquad . \end{array}$$

3 3.1.

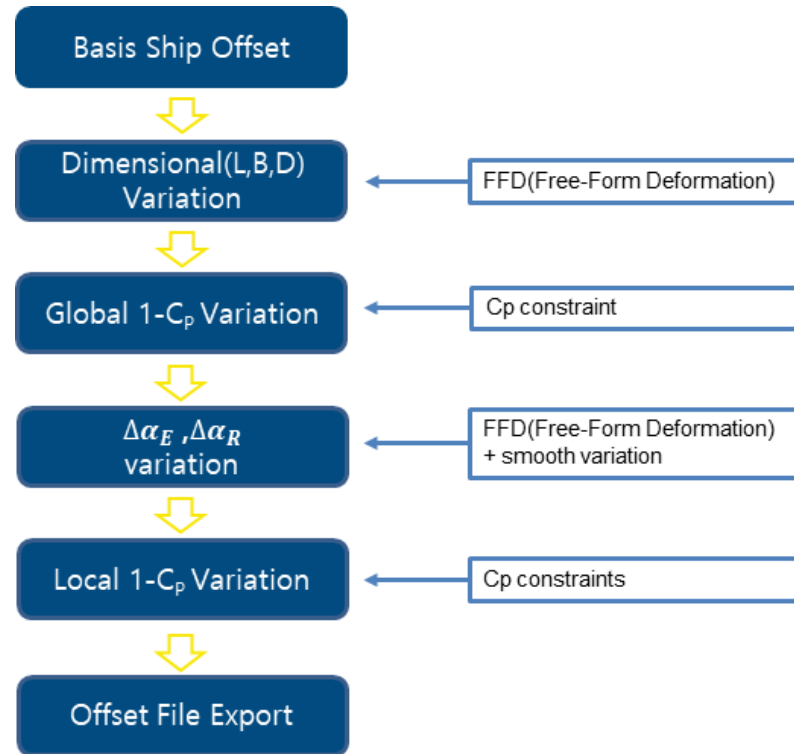


Fig 3.1 Flow chart of the proposed hull form variation method

Fig 3.1

LBD
Min-Max

Free-Form Deformation

$1 - C_P$

가

Min-Max Box

Local $1 - C_P$

가

가

가

KVLCC2 x , y , z
 가 Fig 3.2 .

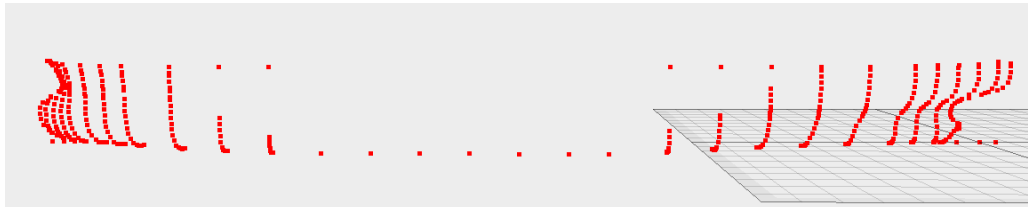


Fig 3.2 KVLCC2 offset data

Fig 3.2

KVLCC2

KCS

section

station

x

가

section

(x,0,0)

(x, Half Breath - Bilge Radius, 0)

(x, Half Breath - Bilge Radius, 0)

(x, Half Breath, Bilge Radius)

1/4

(x, Half Breath, Bilge Radius)

(x, Half Breath, Depth)

. Fig 3.3

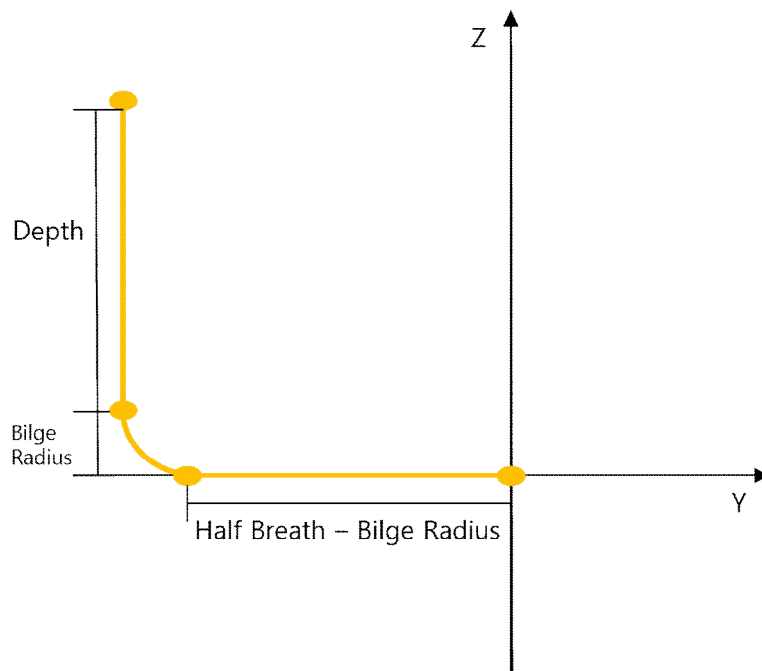


Fig 3.3 Generating midship section line

section

3.3 C_P

Fig 3.4

Fig 3.5

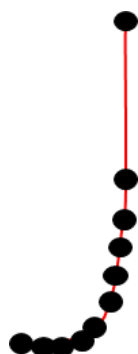
$$y$$


Fig 3.4 Make curve from offset data

Cubic Interpolation

$$\mathbf{Z}$$

Fig 3.4

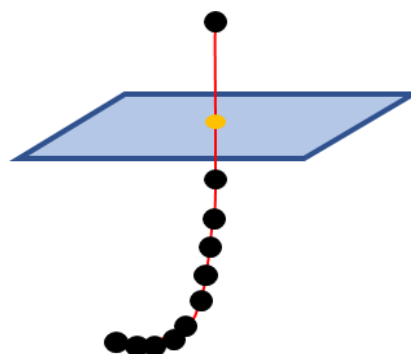


Fig 3.5 The offset where curve
and plane meet

X,

$$y$$
$$C_P$$

X

Fig 3.6

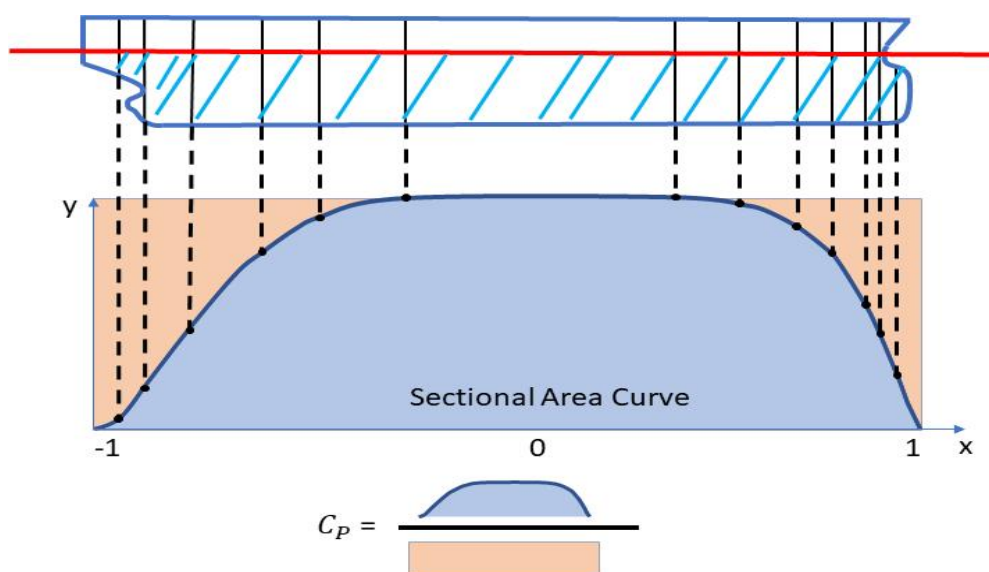
$$C_P$$


Fig 3.6 The method of calculating C_P

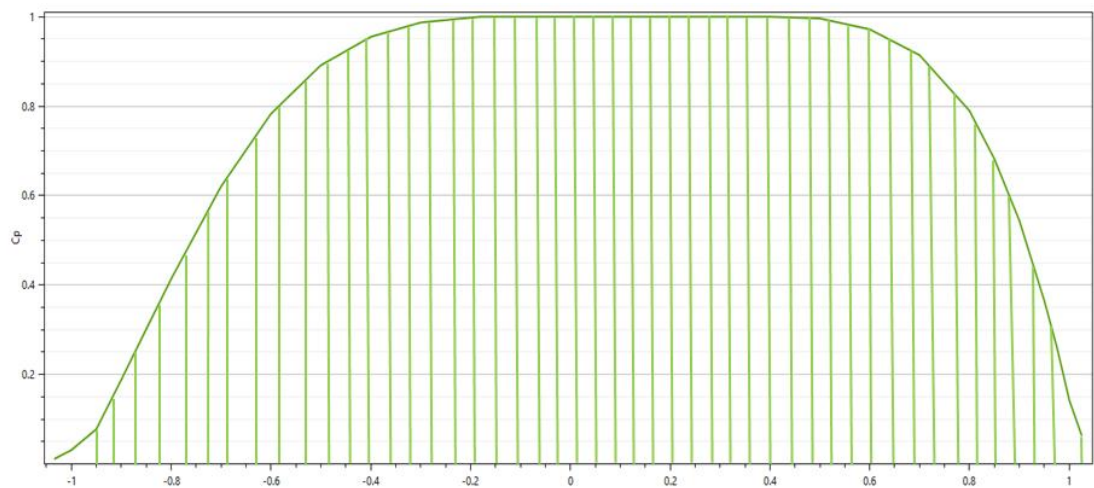


Fig 3.7 The method of calculating Sectional Area Curve

3.4. Free–Form Deformation

LBD

	L,B,D		FFD
LBD		FFD	Min–Max
Box			
FFD			
FFD			
Min–Max Box		x (), y (
), z ()	가		
Min–Max Box		(1) (2) (s,t,u)	
	S,T,U		
	FFD	Min–Max Box	3.6
S 3 , U 5		S 3	
가	, U 5		
	Min–Max Box	가	
(3)			
		(4)	

Table 3.1

KVLCC2

50%

Table 3.2

KCS

, , 50% FFD
 LBD L,B,D
 LBD 가
 $1 - C_P$

Table 3.1 KVLCC2 applying LBD variation

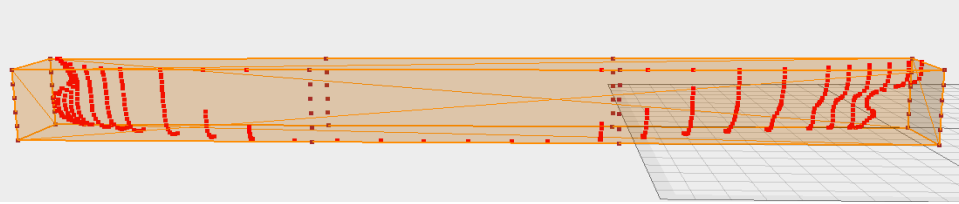
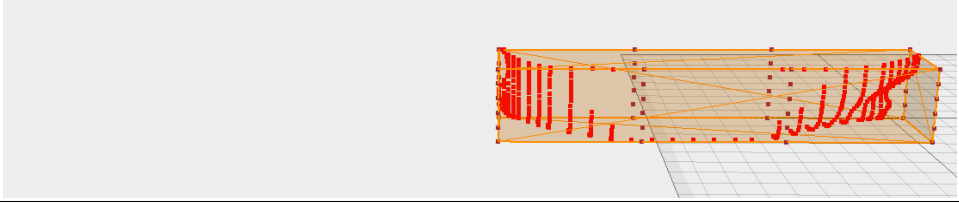
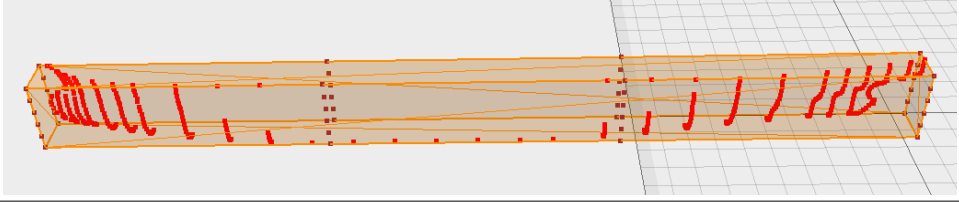
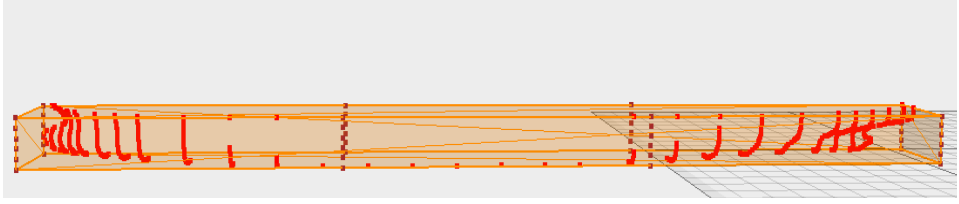
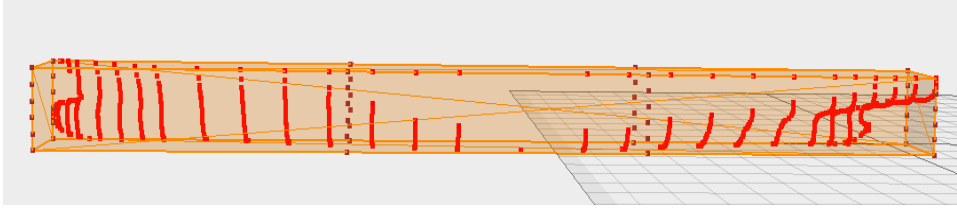
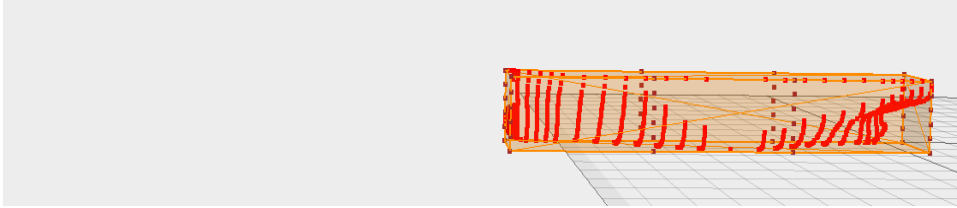
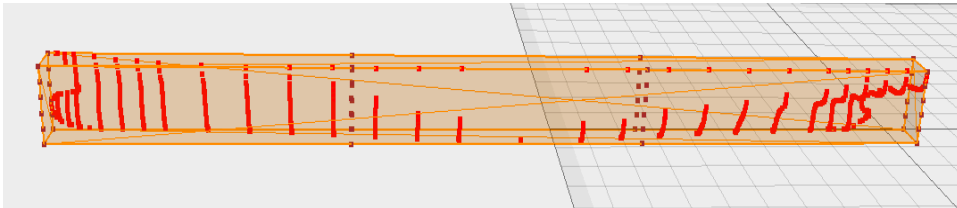
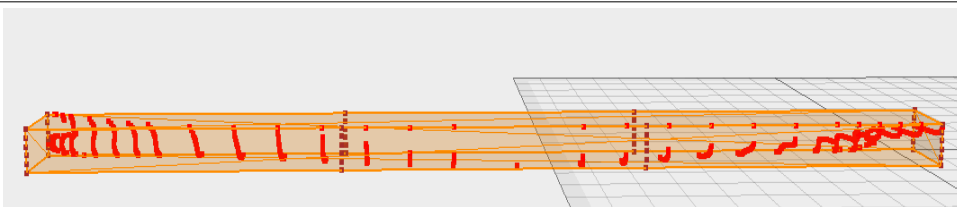
Original KVLCC2 offset

KVLCC2 applying x direction variation

KVLCC2 applying y direction variation

KVLCC2 applying z direction variation


Table 3.2 KCS applying LBD variation

Original KCS offset

KCS applying x direction variation

KCS applying y direction variation

KCS applying z direction variation


3.5 $1-C_P$

LBD

δC_P

(8)

$\delta x_{Pf,a}$

가

(9)

(7)

$1-C_P$

LCB

C_P

C_{Pf}

C_{Pa}

$C_{Pf,a}$

$h_{f,a}$

section

3.5.1 $1-C_P$

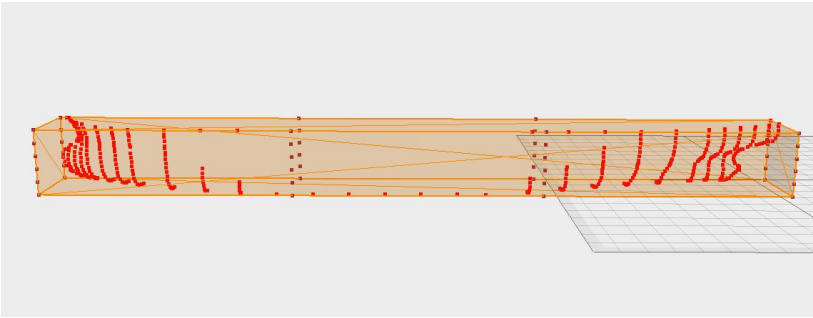


Fig 3.8 KVLCC2 applying 99.7% LBD variation

Fig 3.8	KVLCC2	Min-Max Box	99.7%
		0.80882	0.80745
δC_P		0.001365	

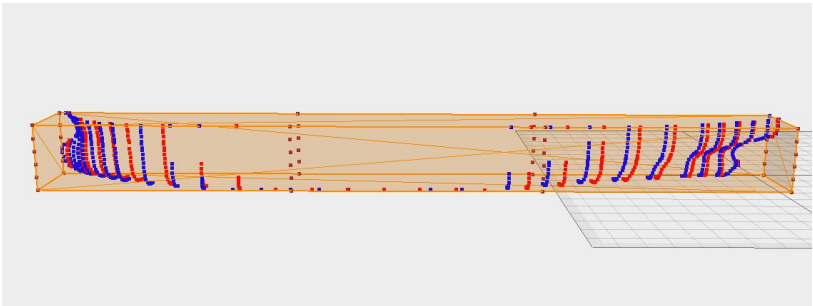


Fig 3.9 KVLCC2 after $1-C_P$ correction

Fig 3.9 $1 - C_P$ 0.80882

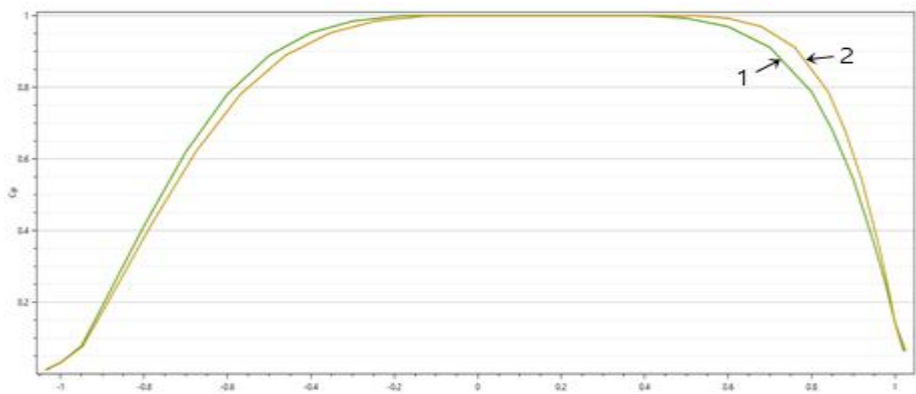


Fig 3.10 Comparison C_P curve before and after $1 - C_P$ correction

Fig 3.10 C_P . 1 C_P
 , 2 C_P .

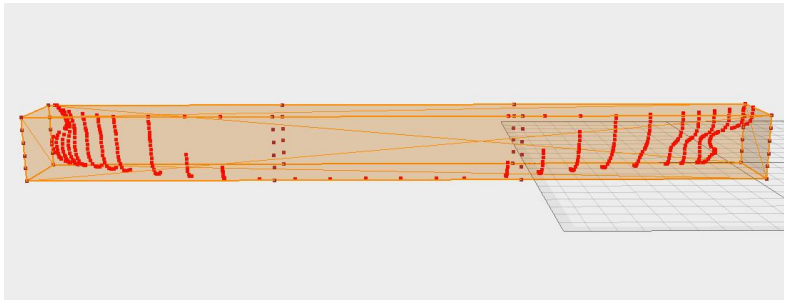


Fig 3.11 KVLCC2 applying 100.5% LBD variation

Fig 3.11 KVLCC2 Min-Max Box 100.5%
 0.80882 0.81024
 δC_P -0.00142 .

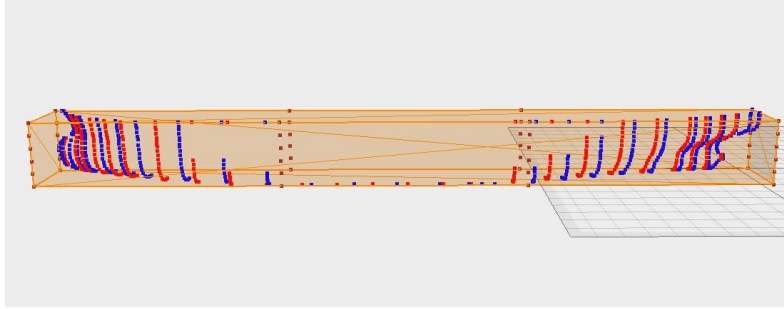


Fig 3.12 KVLCC2 after $1-C_P$ correction

Fig 3.12

$1 - C_P$	C_P	0.80882
-----------	-------	---------

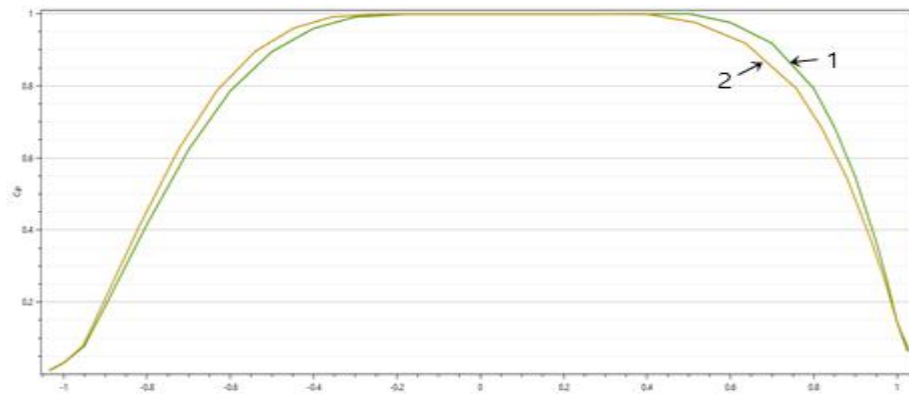


Fig 3.13 Comparison C_P curve before and after $1-C_P$ correction

Fig. 3.13

C_P . 1 C_P

, 2 C_P .

1- C_P KCS KVLCC2 LBD section

3.6 가 ,

L,B,D
가 . 가 가
가
profile line
KVLCC2
profile line
[18]
line 19 station
profile line 3 station
.

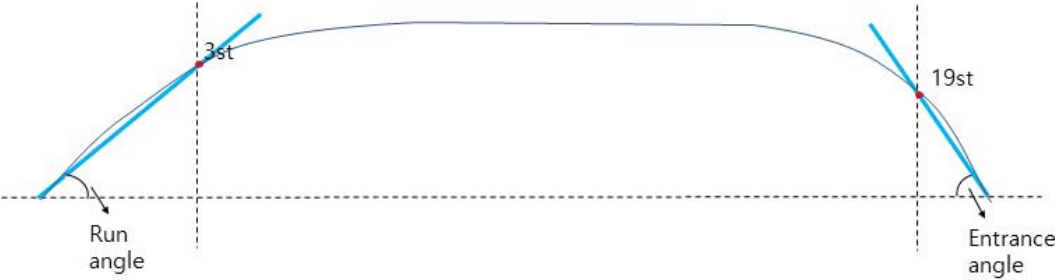


Fig 3.14 Run angle and entrance angle[18]

3.6.1 가 , FFD

가 FFD ,
Min-Max Box X 3 , Z 5 . Fig 3.15
offset , 100% ,
20% .
가 ,
station . Min-Max Box
가 .

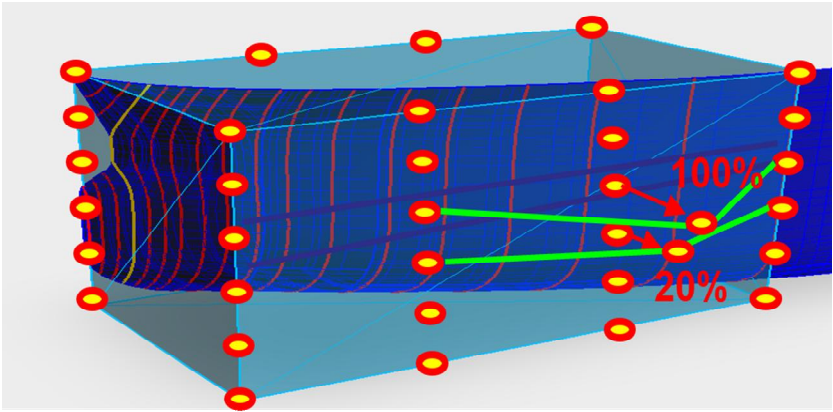


Fig 3.15 FFD method of entrance angle

FFD Min-Max Box 2.1 (4) Box
.
가 .
Box 가
Min-Max Box .
Fig 3.16 θ θ'
.
(4) Y_{draft} y
s,t,u Fig 3.16
Min-Max Box .
Fig 3.15
가 .
y δy (4)
C .

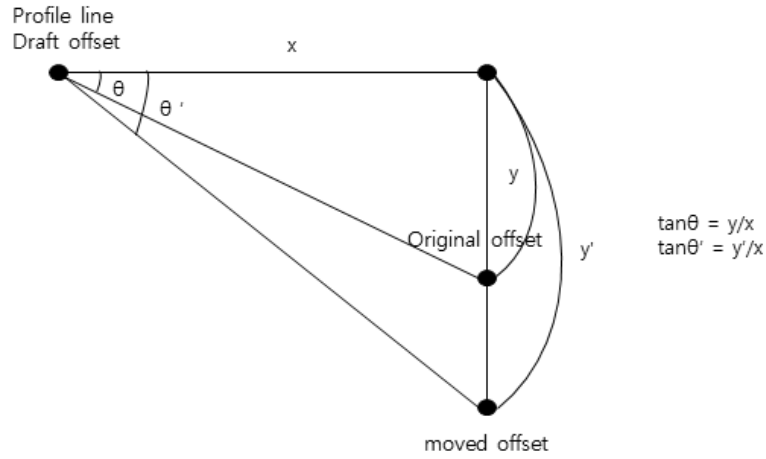


Fig 3.16 Calculation of the moved offset

$$\begin{array}{ccc}
 100\% & & ijk \\
 (P_{ijk} + \delta y), & 20\% & 100\% \\
 z & (P_{ij(k-1)} + 0.2\delta y) \text{가} & . \\
 (11) & & (4)
 \end{array}$$

$$\begin{aligned}
 Y_{\text{draft}} - C &= (1-s)^{l-i} s^i (1-t)^{m-j} t^j (1-u)^{n-k} u^k (P_{ijk} + \delta y) \\
 &+ (1-s)^{l-i} s^i (1-t)^{m-j} t^j (1-u)^{n-(k-1)} u^{(k-1)} (P_{ij(k-1)} + 0.2\delta y)
 \end{aligned} \quad (11)$$

$$\begin{array}{ccc}
 P_{ijk} & P_{ij(k-1)} & (1-s)^{l-i} s^i (1-t)^{m-j} t^j (1-u)^{n-k} u^k P_{ijk} \\
 (1-s)^{l-i} s^i (1-t)^{m-j} t^j (1-u)^{n-(k-1)} u^{(k-1)} P_{ij(k-1)} & & P \\
 (12) & & (11)
 \end{array}$$

$$\begin{aligned}
 Y_{\text{draft}} - C - P &= (1-s)^{l-i} s^i (1-t)^{m-j} t^j (1-u)^{n-k} u^k \delta y \\
 &+ (1-s)^{l-i} s^i (1-t)^{m-j} t^j (1-u)^{n-(k-1)} u^{(k-1)} 0.2\delta y
 \end{aligned} \quad (12)$$

$$\begin{array}{ccc}
 \delta y & (12) & (13) \\
 s, t, u & l, m, n & i, j, k \\
 & (13) &
 \end{array}$$

$$\begin{aligned}
 H &= (1-s)^{l-i} s^i (1-t)^{m-j} t^j (1-u)^{n-k} u^k + 0.2(1-s)^{l-i} s^i (1-t)^{m-j} t^j (1-u)^{n-(k-1)} u^{(k-1)} \\
 &\quad \delta y \\
 (P_{ijk} + \delta y) &\quad (P_{ij(k-1)} + 0.2\delta y) \quad (4) \\
 \text{가} &\quad \text{가}
 \end{aligned}$$

$$X_{\text{ffd}} - \text{C} - \text{P} = \delta y ((1-s)^{l-i} s^i (1-t)^{m-j} t^j (1-u)^{n-k} u^k + 0.2(1-s)^{l-i} s^i (1-t)^{m-j} t^j (1-u)^{n-(k-1)} u^{(k-1)}) \quad (13)$$

$$\frac{X_{\text{ffd}} - \text{C} - \text{P}}{H} = \delta y \quad (14)$$

Fig 3.17 Min-Max Box 25.7 , 28.5 . Fig 3.18 Min-Max Box 58 . 55 control point Min-Max Box .

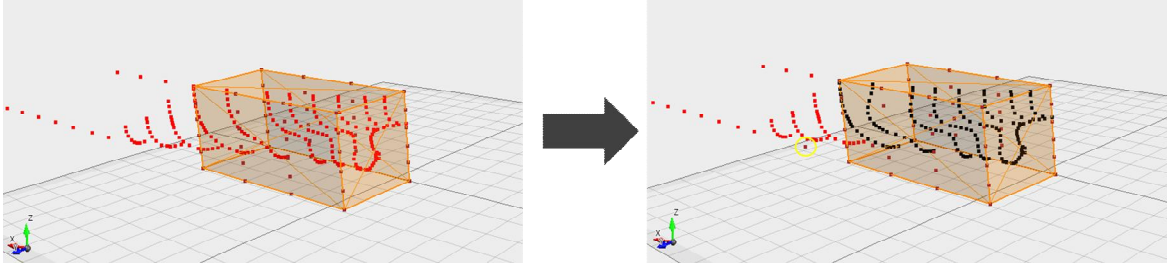


Fig 3.17 Run angle before and after applying FFD

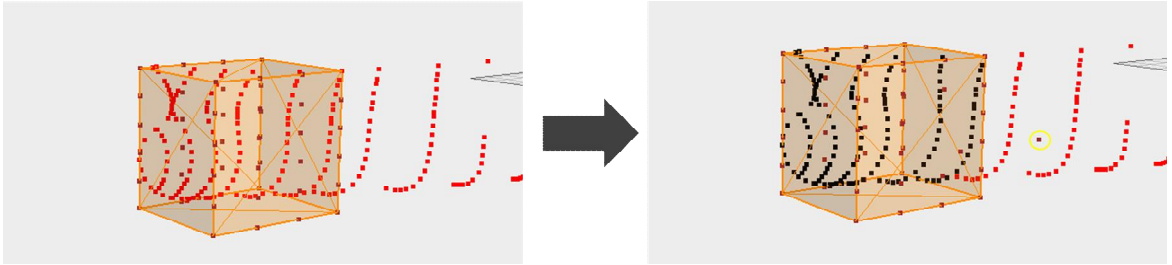


Fig 3.18 Entrance angle before and after applying FFD

, $1 - C_P$
Min-Max Box section section

3.7 Local $1-C_P$

가 , 가
Local $1-C_P$

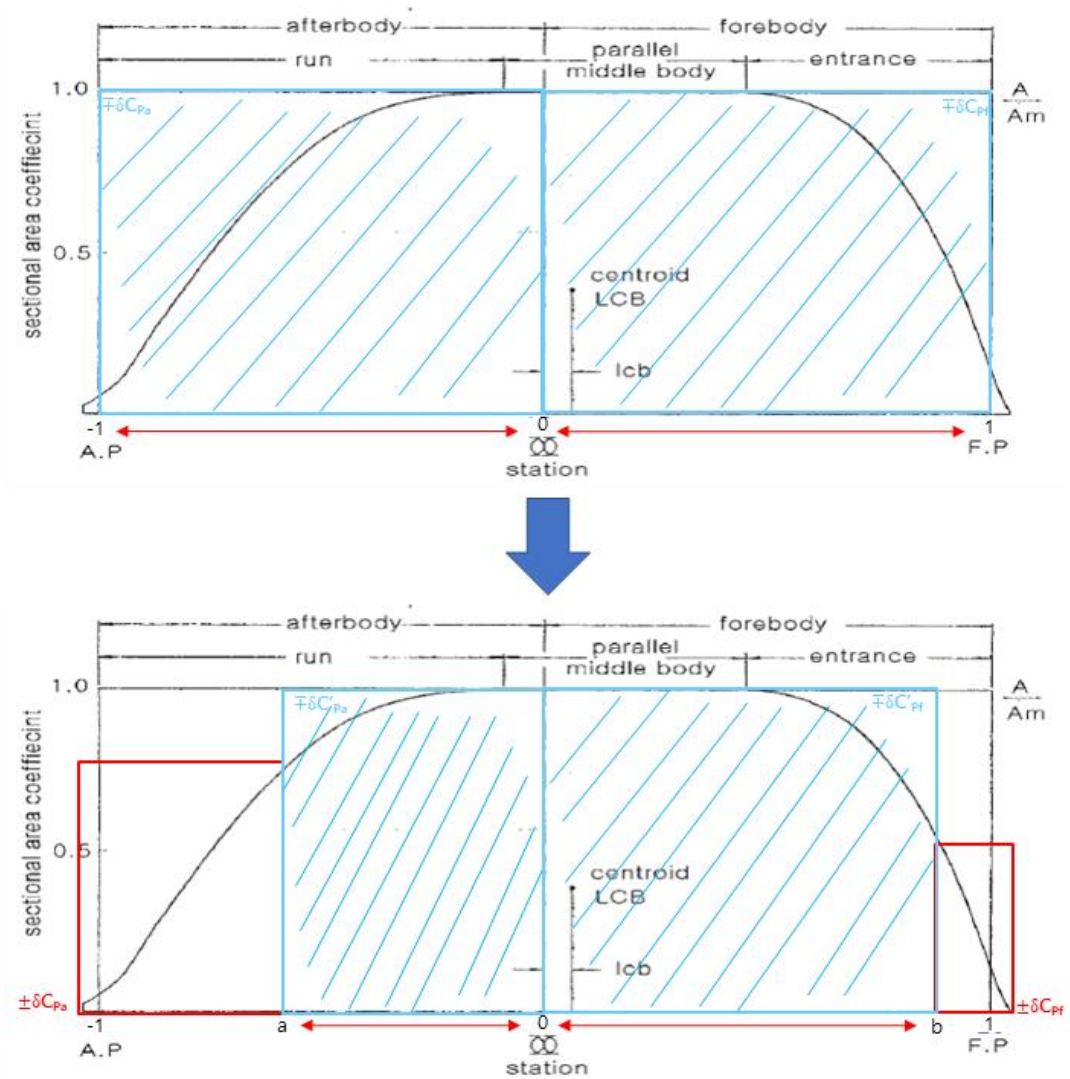


Fig 3.19 Original $1-C_P$ variation and local $1-C_P$ variation

Fig 3.19 $1-C_P$ Local $1-C_P$
 $1-C_P$ ~
1 Local $1-C_P$
Free-Form Deformation

. Local $1 - C_P$

Fig 3.19

가

Fig 3.19

$$(\delta C_P) \quad (15)$$

$$\delta C_P = \frac{\delta \nabla}{L_{BP} \cdot A_M} \quad (15)$$

Fig 3.19

Min-Max Box

가

$$\delta C_P \quad \text{Local } 1 - C_P \quad (16)$$

$\delta \nabla$

$$L_{BP}' \quad (17)$$

$\delta C_P'$

$$\delta \nabla = \delta C_P \cdot L_{BP} \cdot A_M \quad (16)$$

$$\delta C_P' = \frac{\delta \nabla}{L_{BP}' \cdot A_M} \quad (17)$$

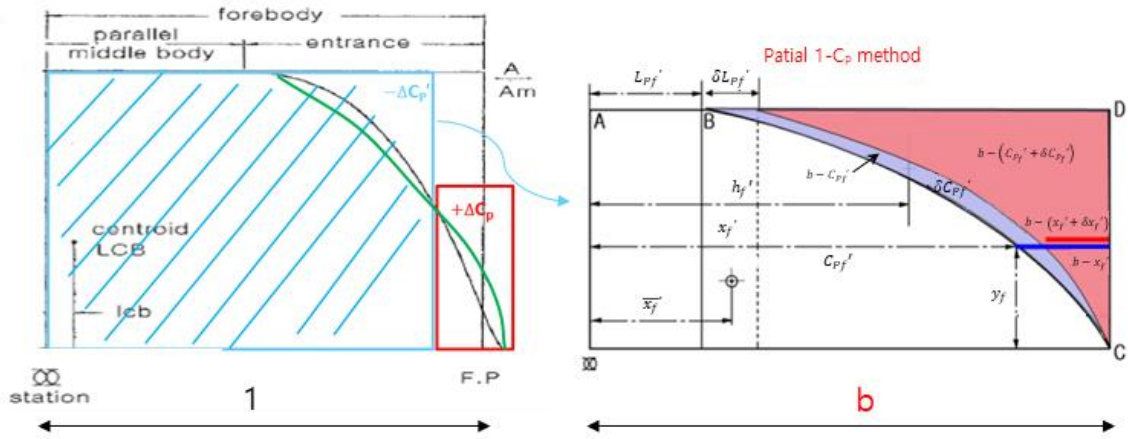


Fig 3.20	Local $1-C_p$	$1-C_p$
	Min-Max Box 4 station	
4 station	a	Min-Max Box
18.5 station	18.5 station	b
(6)	(18),	(19)

$$a - (x_a' + \delta x_a') : a - x_a' = a - (C_{Pa}' + \delta C_{Pa}') : a - C_{Pa}' \quad (18)$$

$$b - (x_f' + \delta x_f') : b - x_f' = b - (C_{Pf}' + \delta C_{Pf}') : b - C_{Pf}' \quad (19)$$

$$\text{section} \quad (20)$$

$$\text{section} \quad (21)$$

$$\delta x_a' = \frac{\delta C_{Pa}'}{a - C_{Pa}'} (a - x_a') \quad (20)$$

$$\delta x_f' = \frac{\delta C_{Pf}'}{b - C_{Pf}'} (b - x_f') \quad (21)$$

$$C_P', \delta C_P', LCB', \delta LCB' \text{가} \quad , \delta C_{Pf,a}' \quad (22) \quad (23)$$

$$\delta C_{Pa}' = \frac{2\{\delta C_P'(h_a' + LCB') + \delta LCB'(C_P' + \delta C_P')\}}{h_f' + h_a'} \quad (22)$$

$$\delta C_{Pf}' = \frac{2\{\delta C_P'(h_a' + LCB') + \delta LCB'(C_P' + \delta C_P')\}}{h_f' + h_a'} \quad (23)$$

$$\delta C_{Pf,a}' \quad h_a' \quad (24) \quad , \quad h_f' \quad (25) \quad .$$

$$h_a' \cong \frac{C_{Pa}'(a - 2\overline{x_a'})}{a - C_{Pa}'} \quad (24)$$

$$h_f' \cong \frac{C_{Pf}'(b - 2\overline{x_f'})}{b - C_{Pf}'} \quad (25)$$

3.7.1 Local 1- C_P

Fig 3.21 105% FFD
0.80882 0.80925 .



Fig 3.21 Increase entrance angle and run angle after applying FFD

Fig 3.22 Local 1- C_P δC_P . Min-Max
Box ,
. 1- C_P 0.80861



Fig 3.22 KVLCC2 corrected with local $1-C_p$

Fig 3.23 C_p 0.80882 C_p 0.80823 95% FFD .

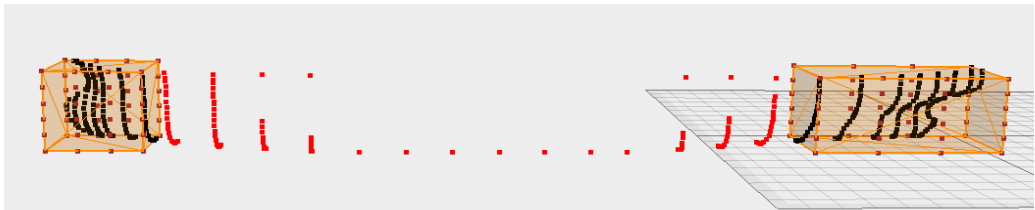


Fig 3.23 Decrease entrance angle and run angle after applying FFD

Fig 3.24 Local $1-C_p$ δC_p . Min-Max Box , $1-C_p$ C_p 0.8089 .



Fig 3.24 KVLCC2 corrected with local $1-C_p$

가

3.7.2 Local $1-C_P$

3.7.1 , Local $1-C_P$ C_P 가 .
Local $1-C_P$. Local $1-C_P$ Min-Max Box section 가 Local $1-C_P$. Fig 3.25
105% FFD . 0.80882
0.80886 . Local $1-C_P$
0.80882 .

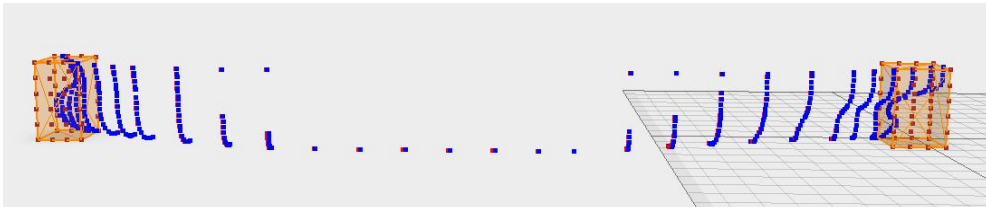


Fig 3.25 KVLCC2 corrected by local $1-C_P$ after applying 105% FFD

Fig 3.26 95% FFD .
0.80882 0.80877 . Local $1-C_P$
0.80882 .

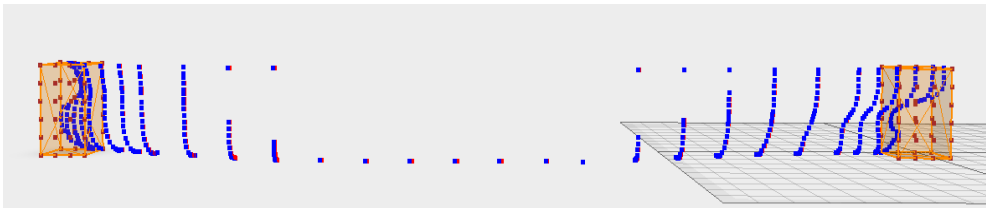


Fig 3.26 KVLCC2 corrected by local $1-C_P$ after applying 95% FFD

Fig 3.27 150% FFD .
0.80882 0.8093 . Local $1-C_P$
0.8088 0.00002 가 .

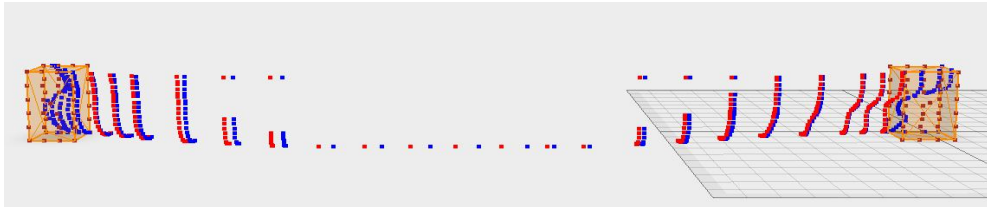


Fig 3.27 KVLCC2 corrected by local $1-C_P$ after applying 150% FFD

Fig 3.28

	0.80882	200% FFD	.
Local $1-C_P$		0.8097	가
0.00004	가	0.80878	
section		$1-C_P$	
	가	가	.

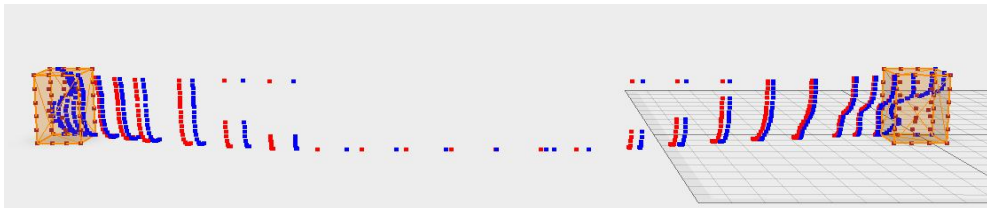


Fig 3.28 KVLCC2 corrected by local $1-C_P$ after applying 200% FFD

Table 3.3 Local $1-C_P$, Table 3.4 Local $1-C_P$

Min-Max Box

Table 3.3 Compare C_P at 3.7.1

		FFD	$1-C_P$	
105%	0.80882	0.8092	0.8086	0.00022
95%	0.80882	0.8082	0.8089	0.00008

Table 3.4 Compare C_P at 3.7.2

		FFD	$1-C_P$	
105%	0.80882	0.80886	0.80882	0
95%	0.80882	0.80877	0.80882	0
150%	0.80882	0.8093	0.8088	0.00002
200%	0.80882	0.8097	0.80878	0.00004

Table 3.3	FFD	Local $1 - C_P$
	.	가
	Local $1 - C_P$	section
.	Min-Max Box	Local $1 - C_P$
section	Table 3.4	가
.		

가 Free-Form Deformation

Local $1 - C_P$ KVLCC2 KCS

Min-Max Box LBD

LBD $1 - C_P$ 가

가 Min-Max Box

Free-Form Deformation , 가

$\pm \delta C_P$

$\mp \delta C_P'$ Local $1 - C_P$

가 0.00008~0.00022 가 Local $1 - C_P$

Min-Max Box

section 가 , 50%~100% 가

가 0.00002~0.00004 가

section

가

“ ”

“ ”

LCB

C_P

, C_P 가

- [1] Sederberg, T.W. and Parry, S.R., "Free-Form Deformation of Solid Geometric Models," Computer Graphics, 20(4), pp. 151-160, 1986.
- [2] Roh, M.I. and Lee, K.Y., Computational Ship Design, Springer, Singapore, pp. 157-160, 2018.
- [3] Kim, H.C., 2004. Parametric Design of Ship Hull Forms with a Complex Multiple Domain Surface Topology. Ph.D. Thesis, Technical University Berlin.
- [4] Lackenby, H., "On the systematic geometrical variation of ship forms," British Shipbuilding Research Association, pp. 289-296, 1950.
- [5] Choi, H.J., Chun, H.H. and Jung, S.H., 2004, "Fundamental Study for the Development of an Optimum Hull Form," Journal of ocean engineering and technology, Vol. 18, No. 3, pp. 32-39.
- [6] Creutz, G., 1977. Curve and Surface Design from Form Parameters by Means of B-Splines. (in German), Ph.D. Thesis, Technical University Berlin.
- [7] Harries, S., 1998, Parametric Design and Hydrodynamic Optimization of Ship Hull Forms, Ph.D. Thesis, Institut fuer Schiffs-und Meerestechnik, Technische Universitaet Berlin, Mensch & Buch Verlag, Berlin.
- [8] Kim, H.C., Lee, K.S. and Kim, S.Y., 1998, "Hull Form Representation using a Hybrid Curve Approximation," The Society of Naval Architects of Korea, Vol. 35, No. 4, pp.118-119.
- [9] Kim, H.J. and Chun, H.H., 2000, "Hull Form Generation of Minimum Wave Resistance by a Nonlinear Optimization Method," Journal of the Society of Naval Architects of Korea, Vol. 37, No. 4, pp. 11-18.
- [10] Choi, H.J., Seo, K.C., Kim, B.E. and Chun, H.H., 2003, "Development of an Optimum Hull Form for a Container Ship with Minimum Wave Resistance," Journal of the Society of Naval Architects of Korea, Vol. 40, No. 4, pp. 8-15.
- [11] Masuda, S and Suzuki, K., 2001, "Experimental Verification of Optimized Hull Form Based on Rankine Source Method," Journal of Soc. N.A.,Japan, Vol.

236, pp. 27–33.

[12] Markov, N.E. and Suzuki, K., 2001, "Hull Form Optimization by Shift and Deformation of Ship Sections," *Journal of Ship Research*, Vol. 45, No. 3, pp. 197–204.

[13] Lee, Y.S. and Choi, Y.B., 2009, "Hull Form Optimization Based on From Parameter Design," *Journal of the Society of Naval Architects of Korea*, Vol. 46, No. 6, pp. 562–568.

[14] Kim, H.C., 2013, "On the Volumetric Balanced Variation of Ship Forms," *Journal of the Society of Naval Architects of Korea*, Vol. 27, No. 2, pp. 1–7.

[15] Park, C.K., 2018, "A Study on the Ship Optimal Design Using Hull Form Variation," *Journal of the Korean Society of Mechanical Technology*, Vol. 20, No. 2, pp. 238–245.

[16] Neu, W.L., Hughes, O., et al., 2000, "A Prototype Tool for Multidisciplinary Design Optimization of Ships," *Ninth Congress of the International Maritime Association of the Mediterranean*, Naples, Italy

[17] Kim, T.H., Choi, H.J., 2017, "Study for the Development of an Optimum Hull Form using One Minus Prismatic," *Journal of the Korean Society of Mechanical Technology*, 19(1), pp 71~76.

[18] Kim, Y.C., et al., 2019, "Prediction of Residual Resistance Coefficient of Low-speed Full Ships using Hull Form Variables and Model Test Results," *Journal of the Society of Naval Architects of Korea*, Vol. 56, No. 5, pp. 447–456.

가
Fig 1 . Visual studio C# ,
Eyeshot .



Fig 1. Procedure of hull form variation

Fig 2 . , δC_P , FFD
Min-Max Box , FFD
Visualization 가 2
Graph C_P .

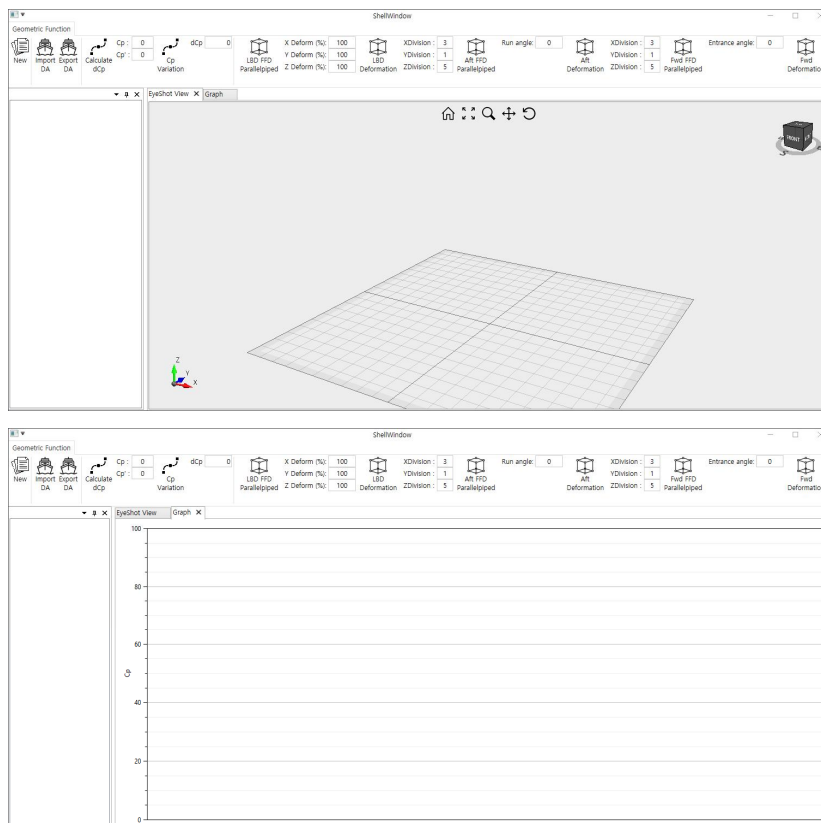


Fig 2. Interface of hull form variation program

Import DA

x,y,z

Visualization

가

Graph

C_P

Fig 3 KVLCC2

가

Fig 4 KVLCC2

C_P

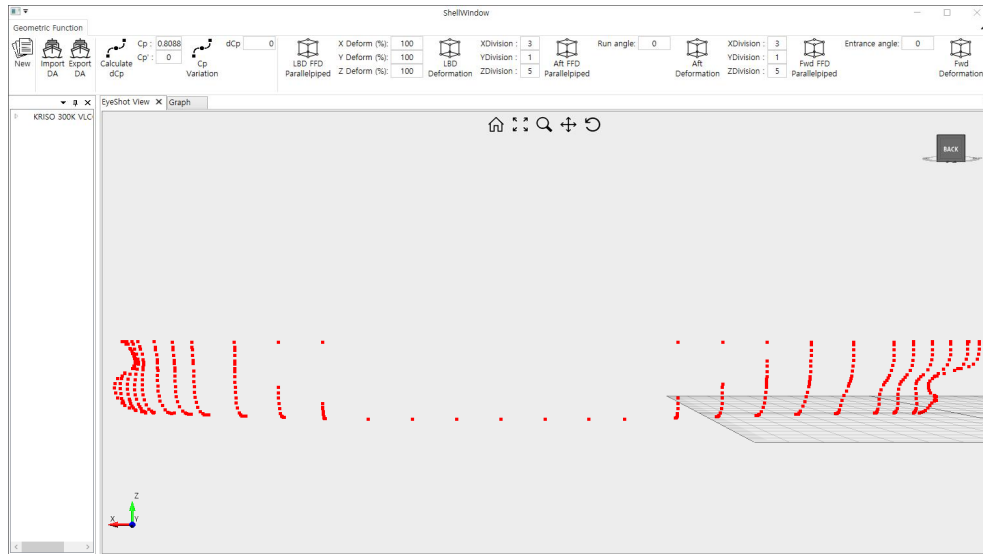


Fig 3. Visualized KVLCC2 offset data

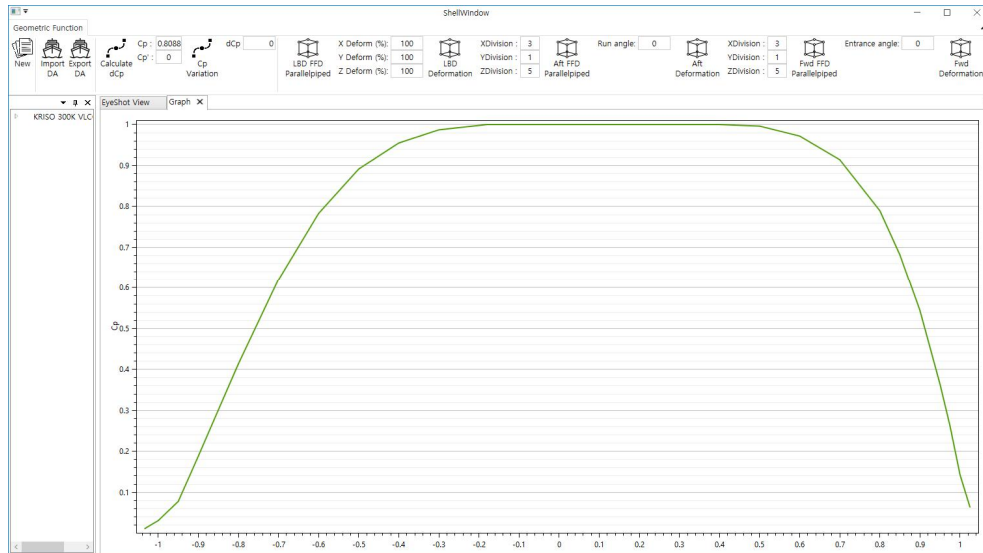


Fig 4. KVLCC2 C_P curve

-LBD
 Min-Max Box . LBD FFD Parallelpipped
 Deform X,Y,Z
 LBD Deformation FFD . Fig 5 KVLCC2
 Min-Max Box .

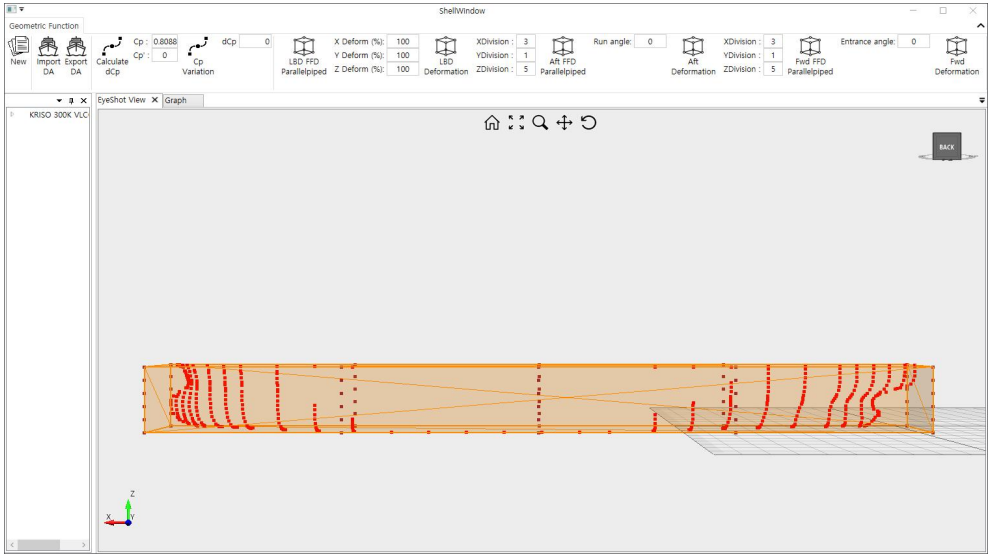


Fig 5. Min-Max Box covering KVLCC2

$-1-C_P$
 Variation dC_P 가 dC_P Cp
 0.0009 0.8088 0.8097
 . Fig 7 C_P C_P
 .

-LBD
 Export DA .

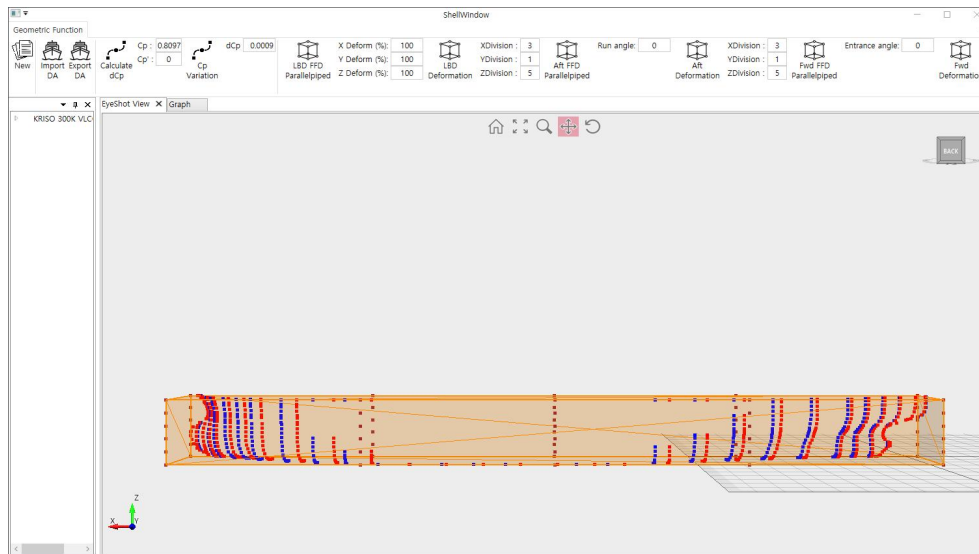


Fig 6. Variated KVLCC2 offset

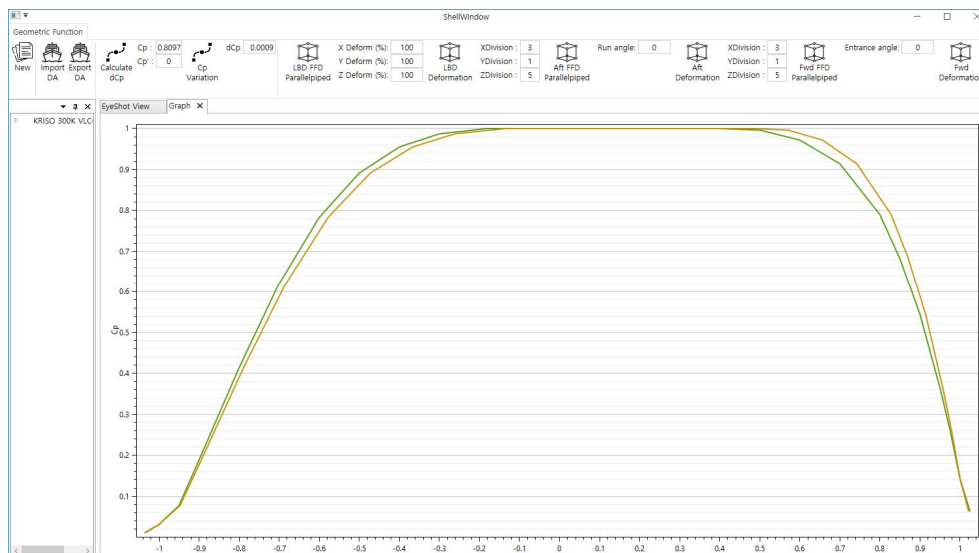


Fig 7. Variated KVLCC2 C_p Curve

- 가 ,
 LBD Aft FFD Parallelipped
 Min-Max Box . Aft Deformation
 가 Run angle .
 Run angle Aft Deformation
 Min-Max Box . 가
 . Fig 8 가 24.6° 24.8°
 59° 59.2° .

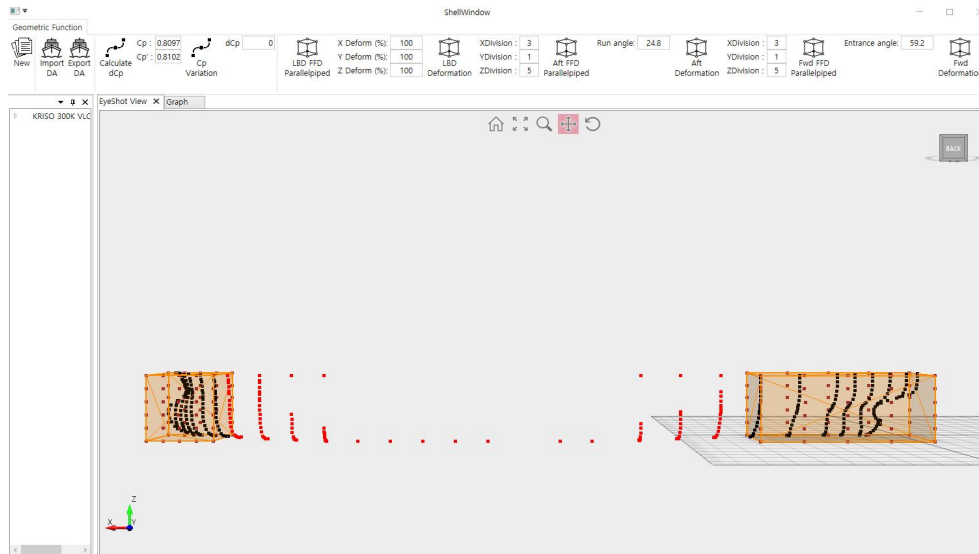


Fig 8. KVLCC2 varied run angle and after angle

- Local $1 - C_P$
 0.8097 가
 0.8102가 C_p' . Calculate dCp
 C_p' dCp가 . C_p variation
 Local $1 - C_P$. Fig 9 Min-Max Box
 section x
 0.8101 0.0004 . C_P Fig 10



Fig 9. KVLCC2 offset performed Local $1 - C_P$

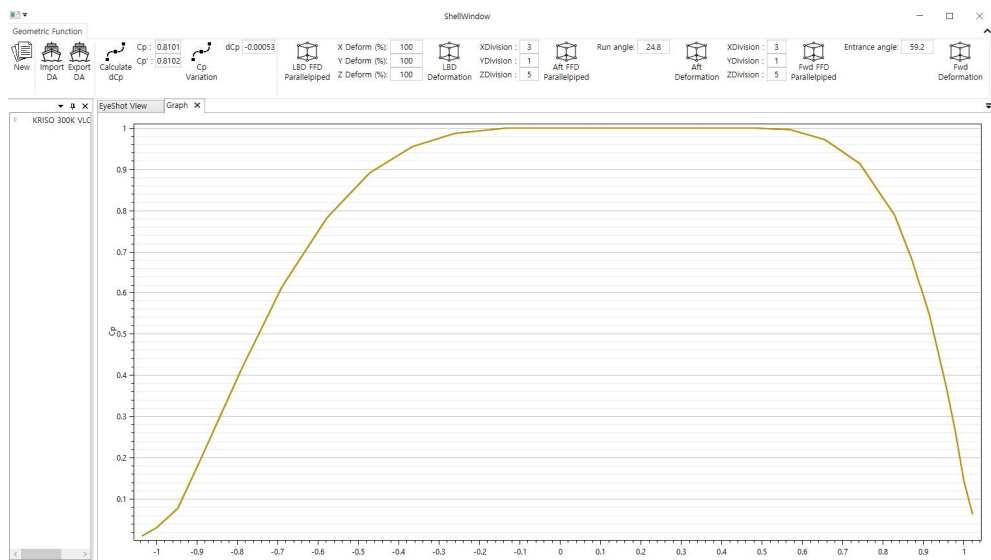


Fig 10. KVLCC2 C_P curve performed Local $1-C_P$

—

Local $1-C_P$

Export DA

Entrance and Run Angles Variation Method of Hull Form Preserving the Prismatic Coefficient

Eunyoung Son

Department of Naval architecture and Ocean engineering, University of Ulsan

ABSTRACT

There are several methods of hull form variation for initial ship design, such as offset variation, lines variation, and hull form variable variation. In general, this hull form variation is done manually, and different results are obtained according to the designer's know-how. This study proposes a method of converting using the Free-Form Deformation method for entrance angle and run angle among the variables capable of converting hull form. The Free-Form Deformation is method transforming shapes. The variation using Free-Form Deformation method has the advantage of being able to smoothly convert the overall shape of the object to be variated, so the local variation is smoothly controlled when a designer manually transforms. However, if the Free-Form Deformation method is used the variate entrance angle and run angle of the bow and stern, the prismatic coefficient, which is a constraint, will be changed. Therefore, in order to obtain the same prismatic coefficient as before variation, a method of correcting the prismatic coefficient converted $1-C_P$ variation while maintaining the entrance angle and run angle was proposed and the result was verified. The proposed method can shorten the time to generate various hull form data for finding optimal hull form. In addition, it will be helpful to strengthen the competitiveness of small and medium-sized shipbuilders who lack hull form variation technology as it is possible to propose optimal hull form.